Measurement of L-shell fluorescence yields of some elements in the atomic range $65 \leqslant Z \leqslant 74$ using photoionization

Önder Şimşek, Oğuz Doğan, Ümit Turgut, and Mehmet Ertuğrul
Department of Physics, K. K. Education Faculty, Atatürk University, 25240 Erzurum, Turkey
(Received 22 August 1997)

L-shell fluorescence yields were measured for seven elements Tb, Dy, Ho, Er, Yb, Ta, and W using a Ge(Li) detector. The targets were excited using 59.5-keV γ rays from Am^{241} radioactive source of strengths 100 mCi. The results obtained were compared with the theoretical values and other measured values. It is shown that the present results are in good agreement with earlier experimental and theoretical results. [S1050-2947(98)01908-8]

PACS number(s): 32.30.Rj

INTRODUCTION

The fluorescence yield of an atomic shell or subshell is defined as the probability that a vacancy in that shell or subshell is filled through a radiative transition. The fluorescence yield of a shell is equal to the number of photons emitted when vacancies in the shell are filled, divided by the number of primary vacancies in the shell. The knowledge of fluorescence yields of the L shell has wide interdisciplinary applications in nuclear and atomic measurements. Bambynek *et al.* [1] have fitted selected experimental values of K-, L-, and M-shell fluorescence yields. Hubbell *et al.* [2] have reviewed K-, L-, and higher atomic-shell x-ray fluorescence yields covering the period 1978–1993. An annotated bibliography of x-ray fluorescence yield measurements, analyses, fits, and tables from 1978–1993 and the comparisons of the fluorescence yields, ω_K, $\overline{\omega}_L$, and $\overline{\omega}_M$ based on measurements, and on theoretical models are also given. Values of ω_K, $\overline{\omega}_L$, and $\overline{\omega}_M$ fitted to standard empirical parametric formulations and selected well-characterized measured ω_K, $\overline{\omega}_L$, and $\overline{\omega}_M$ results restricted to the period 1978–1993 are listed. Krause [3] has determined K-shell and L_1-, L_2-, and L_3-subshell fluorescence yields for all elements $5 \leqslant Z \leqslant 110$.

In recent years, L-shell fluorescence yields for many elements were measured by several authors [4–6]. Singh *et al.* [4] have measured L-shell fluorescence yields of 27 elements: Ba, La, Ce, Pr, Nd, Sm, Eu, Gd, Tb, Dy, Ho, Er, Tm, Yb, Lu, Hf, Ta, W, Re, Ir, Pt, Au, Tl, Pb, Bi, Th, and U. Mann *et al.* [5] have determined L fluorescence yields 22 elements: La, Ce, Pr, Nd, Sm, Eu, Gd, Tb, Dy, Ho, Er, Yb, Lu, Ta, W, Au, Hg, Tl, Pb, Bi, Th, and U. Ertuğrul [6] has measured L-shell fluorescence yields of 11 elements: La, Ce, Pr, Nd, Sm, Eu, Gd, Tb, Dy, Ho, and Er.

In the present work, L-shell fluorescence yields of seven elements (Tb, Dy, Ho, Er, Yb, Ta, and W) were measured by using photoionization. The targets were ionized using 59.5-keV γ rays from 100-mCi Am^{241} and emitted L-shell x rays were detected with a Ge(Li) detector.

EXPERIMENTAL METHOD

The experimental setup is shown in Fig. 1. 59.5-keV γ rays from an Am^{241} source are collimated on targets, each of thickness 100–300 $\mu g/cm^2$ of Tb, Dy, Ho, Er, Yb, Ta, and W. All the targets have L-edge energies lower than 59.5 keV. The fluorescent x rays produced due to the interactions of the incoming photons with L-shell electrons of the target elements are measured with a Ge(Li) detector (Be window thickness of 12.5 μm and resolution of 190 eV at 5.96 keV) and complied with the ND 66B multichannel analyzer system. The L-shell x-ray spectrum of Ta is shown in Fig. 2.

The L-shell x-ray counting rate from the target of the elements under study and the scattered radiation counting rate from the carbon target, as measured by the detector, are given by

$$N(L) = R \frac{\Omega_1}{4\Pi} \frac{N_A}{M_{(L)}} t_{(L)} W_i \beta_{(L)} (\sigma_L + \eta_{KL}\sigma_K) \frac{\Omega_2}{4\Pi} \varepsilon_{(L)} \overline{\omega}_L \tag{1}$$

and

$$N(\mathrm{C}) = R \frac{\Omega_1}{4\Pi} \frac{N_A}{M_{(\mathrm{C})}} t_{(\mathrm{C})} \beta_{(\mathrm{C})} \frac{d\sigma_{KN}(90°)}{d\Omega} S(x,Z) \Omega_2 \varepsilon_{(\mathrm{C})}. \tag{2}$$

Ω_1 is source-target solid angle, W_i is the concentration in the target of i element, N_A is Avogadro's number, $M_{(L)}$ and $M_{(\mathrm{C})}$ are the atomic weight of the target element and carbon, $t_{(K)}$ and $t_{(\mathrm{C})}$ are the thickness of the target and C, σ_L is the

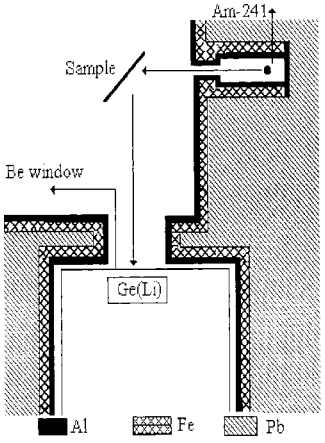

FIG. 1. Experimental setup.

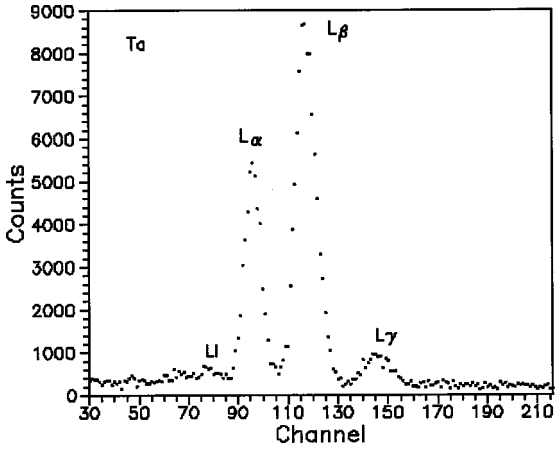

FIG. 2. *L*-shell x-ray spectrum of Ta.

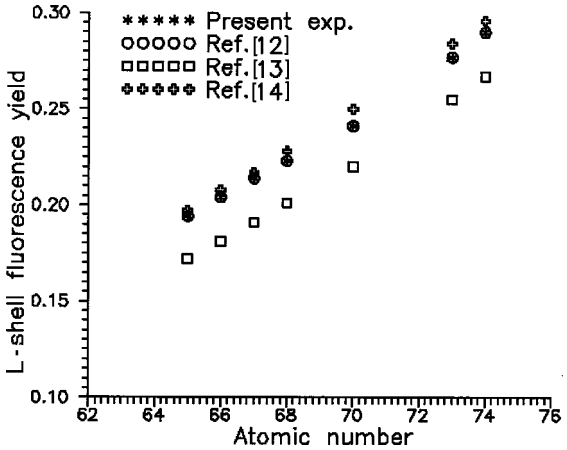

FIG. 3. *L*-shell x-ray fluorescence yield curve versus atomic number.

L-shell photoelectric cross section of the element at the excitation energy of 59.5 keV, $\bar{\omega}_L$ is the *L*-shell fluorescence yield, Ω_2 is the target-detector solid angle, $\varepsilon_{(L)}$ and $\varepsilon_{(\mathrm{C})}$ are the detector efficiencies at the fluorescent and scattered x-ray energies, $\beta_{(L)}$ and $\beta_{(\mathrm{C})}$ are the absorption correction factor of the fluorescent target and C target, $d\sigma_{KN}(90°)/d\Omega$ is the Klein-Nishia differential cross section, and $S(x,Z)$ is the incoherent scattering factor of C. From Eqs. (1) and (2), $\bar{\omega}_L$ can be resolved,

$$\bar{\omega}_L = \frac{M_L}{M_{\mathrm{C}}}\frac{t_{(\mathrm{C})}}{t_{(L)}}\frac{\beta_{(\mathrm{C})}}{\beta_{(L)}}\frac{\varepsilon_{(\mathrm{C})}}{\varepsilon_{(L)}}\frac{N_{(L)}}{N_{(\mathrm{C})}}\frac{4\pi}{W_i(\sigma_L+\eta_{KL}\sigma_K)} \times\frac{d\sigma_{KN}(90°)}{d\Omega}S(x,Z). \tag{3}$$

The $N_{(L)}$ and $N_{(C)}$ values are determined from the photopeak and scattered peak areas at the same counting geometry. The σ_L and σ_K values are the photoionization cross sections of the *L* and *K* shells. The σ_L and σ_K values were taken from table of Scofield [7]. η_{KL} is the vacancy transfer probability. The η_{KL} value was determined using

$$\eta_{KL1}=\frac{1}{\Gamma(K)}[\Gamma_R(KL_1)+2\Gamma_A(KL_1L_1)+\Gamma_A(KL_1L_2) +\Gamma_A(KL_1L_3)+\Gamma_A(KL_1X)], \tag{4}$$

TABLE I. σ_L, σ_K, and $d\sigma_{\mathrm{inc}}(\theta)/d\Omega$ (for carbon) values at 59.5 keV and η_{KL} values.

Element	σ_L (b/atom)	σ_K (b/atom)	η_{KL}	$\frac{d\sigma_{\mathrm{inc}}(\theta)}{d\Omega}$ (for carbon) (b/atom sr)
^{65}Tb	443.50	2612.9	0.848	0.193
^{66}Dy	473.44	2743.1	0.846	
^{67}Ho	504.86	2889.3	0.843	
^{68}Er	537.85	3039.2	0.840	
^{70}Yb	608.77	0	0.836	
^{73}Ta	727.95	0	0.829	
^{74}W	771.38	0	0.827	

$$\eta_{KL2}=\frac{1}{\Gamma(K)}[\Gamma_R(KL_2)+2\Gamma_A(KL_2L_2)+\Gamma_A(KL_1L_2) +\Gamma_A(KL_2L_3)+\Gamma_A(KL_2X)], \tag{5}$$

$$\eta_{KL3}=\frac{1}{\Gamma(K)}[\Gamma_R(KL_3)+2\Gamma_A(KL_3L_3)+\Gamma_A(KL_1L_3) +\Gamma_A(KL_2L_3)+\Gamma_A(KL_3X)] \quad (x=M,N,O), \tag{6}$$

$$\eta_{KL}=\Sigma\,\eta_{KLi}, \tag{7}$$

where Γ_R and Γ_A are the radiative and Auger partial widths corresponding to the transitions between the shells in the parentheses and Γ is the total level width. In these evaluations, *K*-shell radiactive transition rates based on the relativistic DSH model tabulated by Scofield [8] and the Auger transition rates based on the RDHS model calculated in the *jj*-coupling scheme [9] were used.

The differential Klein-Nishina cross section per electron $[d\sigma_{KN}(90°)/d\Omega]$ is calculated by the well-known Klein-Nishina expression [10]. The function of $S(x,Z)$ versus $x=\sin(\theta/2)/\lambda$ was determined for C from the table of Hubbell *et al.* [10]. The self-absorption correction factor for emitted *L*-shell x rays was determined by

$$\beta_{(L)}=\frac{1-\exp\left[-\left(\frac{\mu_\gamma}{\cos\theta}+\frac{\mu_L}{\cos\phi}\right)t_L\right]}{\left(\frac{\mu_\gamma}{\cos\theta}+\frac{\mu_L}{\cos\phi}\right)t_L}, \tag{8}$$

where μ_γ and μ_L are the total attenuation coefficients [11] at primary γ and emitted *L*-shell x-ray energies and θ $(=45°)$ and ϕ $(=45°)$ are the angles with the sample normal primary and emitted *L*-shell x rays. The $\beta_{(C)}$ value is similar to that in Eq. (4),

$$\beta_{(\mathrm{C})}=\frac{1-\exp\left[-\left(\frac{\mu_{\gamma(\mathrm{C})}}{\cos\theta}+\frac{\mu_{s(\mathrm{C})}}{\cos\phi}\right)t_{\mathrm{C}}\right]}{\left(\frac{\mu_{\gamma(\mathrm{C})}}{\cos\theta}+\frac{\mu_{s(\mathrm{C})}}{\cos\phi}\right)t_{\mathrm{C}}}, \tag{9}$$

TABLE II. L-shell x-ray fluorescence yield of elements Tb, Dy, Ho, Er, Yb, Ta, and W.

Element	Present Expt.	Other Expt.	Theory	Fit values
^{65}Tb	0.182(10)	0.192(6)[a]	0.194[d]	0.184[g]
		0.168(10)[b]	0.172[e]	0.172[h]
		0.175(14)[c]	0.197[f]	0.172[i]
^{66}Dy	0.190(9)	0.199(6)[a]	0.204[d]	0.194[g]
		0.175(10)[b]	0.181[e]	0.182[h]
		0.174(9)[c]	0.207[f]	0.182[i]
^{67}Ho	0.200(10)	0.217(6)[a]	0.214[d]	0.205[g]
		0.193(10)[b]	0.191[e]	0.192[h]
		0.191(14)[c]	0.217[f]	
^{68}Er	0.208(6)	0.223(7)[a]	0.223[d]	0.215[g]
		0.205(10)[b]	0.201[e]	0.202[h]
		0.207(14)[c]	0.228[f]	
^{70}Yb	0.235(8)	0.239(7)[a]	0.241[d]	0.236[g]
		0.228(10)[b]	0.220[e]	0.223[h]
			0.250[f]	
^{73}Ta	0.252(11)	0.274(8)[a]	0.277[d]	0.269[g]
		0.254(12)[b]	0.255[e]	0.257[h]
			0.284[f]	0.266[i]
^{74}W	0.283(18)	0.285(8)[a]	0.290[d]	0.280[g]
		0.272(13)[b]	0.267[e]	0.269[h]
			0.296[f]	

[a]Reference [4].
[b]Reference [5].
[c]Reference [6].
[d]Reference [12].
[e]Reference [13].
[f]Reference [14].
[g]Reference [2].
[h]Reference [15].
[i]Reference [1].

where $\mu_{\gamma(\mathrm{C})}$ is the absorption coefficient of carbon at the energy of the incident γ rays, $\mu_{s(\mathrm{C})}$ is the absorption coefficient of carbon at the scattered photon energy calculated by using the Compton relation and a scattering angle of 90°. The detector efficiency was determined with calibrated radioisotope sources of Am^{241}, Ba^{133}, and Mn^{55} using

$$\varepsilon(E)=\frac{4\pi N_E}{\Omega_0 T R P_E}, \tag{10}$$

where N_E is the net count under the photopeak in the time of T, Ω_0 is the solid angle, R is the radioactive decay rate, and P_E is the emission probability of photon at the E energy.

RESULTS AND DISCUSSION

In this work the L-shell fluorescence yield of some elements was measured using a different method. In the method the L-shell x-ray counting rate from the target [Eq. (1)] and the scattered radiation counting rate from the carbon target [Eq. (2)] are measured at the same geometry. From these equations, L-shell fluorescence yield $\overline{\omega_L}$, is resolved [Eq. (3)]. In this method, the value of $\overline{\omega_L}$ is independent of the primary photon flux and the source-target-detector geometry factor. In these calculations, the L- and K-shell photoionization cross sections of Tb, Dy, Ho, Er, Yb, Ta, and W, the differential Compton cross section of carbon, and the K- to L-shell vacancy transfer probabilities of Tb, Dy, Ho, Er, Yb, Ta, and W were used and are shown in Table I. The present experimental results of L-shell fluorescence yields are given in Table II. In addition, the present and other results are fitted versus atomic number and are shown in Fig. 3. It can be seen from Table I and Fig. 3 that the present results are in good agreement with the experimental uncertainties with the earlier experimental and theoretical reports. According to the values of Hubbell *et al.* [2], the errors in the measured L-shell fluorescence yield are estimated to be less than 7% and 10% for this method. This error arises due to the uncertainties in various physical parameters, namely, the error in the evaluation of area under the L-shell x-ray peaks, target thickness, absorption correction factor, and detector efficiency.

[1] W. Bambynek, B. Crasemann, R. W. Fink, H. U. Freund, H. Mark, C. D. Swift, R. E. Price, and P. V. Rao, Rev. Mod. Phys. **44**, 716 (1972).
[2] J. H. Hubbell, P. N. Trehan, N. Singh, B. Chand, D. Mehta, M. L. Garg, R. R. Garg, S. Singh, and S. Puri, J. Phys. Chem. Ref. Data **23**, 339 (1994).
[3] M. O. Krause, J. Phys. Chem. Ref. Data **8**, 307 (1979).
[4] S. Singh, D. Mehta, R. R. Garg, S. Kumar, M. L. Garg, N. Singh, P. C. Mangal, J. H. Hubbell, and P. N. Trehan, Nucl. Instrum. Methods Phys. Res. B **51**, 5 (1990).
[5] K. S. Mann, N. Singh, R. Mittal, K. L. Allawadhi, and B. S. Sood, J. Phys. B **23**, 3521 (1990).
[6] M. Ertuğrul, Z. Phys. D **38**, 91 (1996).
[7] J. H. Scofield, Lawrence Livermore Laboratory Report No. 513626, 1973 (unpublished).
[8] J. H. Scofield, At. Data Nucl. Data Tables **14**, 121 (1974).
[9] M. H. Chen, B. Crasemann, and H. Mark, At. Data Nucl. Data Tables **24**, 13 (1979).
[10] J. H. Hubbell, W. J. Viegele, E. A. Briggs, R. T. Brown, D. T. Cromer, and R. J. Howerton, J. Phys. Chem. Ref. Data **4**, 471 (1975).
[11] J. H. Hubbell and S. M. Seltzer, NISTIR Report No. 5632, 1995 (unpublished).
[12] S. Puri, D. Mehta, B. Chand, N. Singh, and P. N. Trehan, X-Ray Spectrom. **22**, 358 (1993).
[13] D. D. Cohen, Nucl. Instrum. Methods Phys. Res. B **22**, 55 (1987).
[14] I. V. Mitchell and K. M. Barfood, Nucl. Sci. Appl. **1**, 99 (1981).
[15] J. H. Hubbell, NISTIR Report No. 89-4144, 1989 (unpublished).